The Astrophysical Journal Letters, 876:L4 (6pp), 2019 May 1 https://doi.org/10.3847/2041-8213/ab18a1

Potential Gravitational-wave and Gamma-ray Multi-messenger Candidate from 2015 October 30

Alexander H. Nitz [1,2], Alex B. Nielsen [1,2], and Collin D. Capano [1,2]
[1] Max-Planck-Institut für Gravitationsphysik (Albert-Einstein-Institut), D-30167 Hannover, Germany; alex.nitz@aei.mpg.de
[2] Leibniz Universität Hannover, D-30167 Hannover, Germany
Received 2019 February 26; revised 2019 April 11; accepted 2019 April 12; published 2019 April 26

Abstract

We present a search for binary neutron star (BNS) mergers that produced gravitational waves during the first observing run of the Advanced Laser Interferometer Gravitational-Wave Observatory (LIGO), and gamma-ray emission seen by either the *Swift*-Burst Alert Telescope (BAT) or the *Fermi*-Gamma-ray Burst Monitor (GBM), similar to GW170817 and GRB 170817A. We introduce a new method using a combined ranking statistic to detect sources that do not produce significant gravitational-wave or gamma-ray burst candidates individually. The current version of this search can increase by 70% the detections of joint gravitational-wave and gamma-ray signals. We find one possible candidate observed by LIGO and *Fermi*-GBM, 1-OGC 151030, at a false alarm rate of 1 in 13 yr. If astrophysical, this candidate would correspond to a merger at 187^{+99}_{-87} Mpc with source-frame chirp mass of $1.30^{+0.02}_{-0.03}\,M_{\odot}$. If we assume that the viewing angle must be $<30^{\circ}$ to be observed by *Fermi*-GBM, our estimate of the distance would become 224^{+88}_{-78} Mpc. By comparing the rate of BNS mergers to our search-estimated rate of false alarms, we estimate that there is a 1 in 4 chance that this candidate is astrophysical in origin.

Key words: gamma-ray burst: general – gravitational waves – stars: neutron

1. Introduction

The detection of the binary neutron star (BNS) coalescence GW170817 (Abbott et al. 2017b) was a watershed moment in astronomy. In a triumph for multi-messenger astronomy, gravitational-wave (GW) observations turned what would otherwise have been a relatively unremarkable gamma-ray burst (GRB) detection by the *Fermi*-Gamma-ray Burst Monitor (GBM) into one of the most studied astronomical transients of all time (Abbott et al. 2017c; Goldstein et al. 2017). The observation of GW170817 immediately raised the question of whether other coincident detections were possible in archival data that had previously been missed. The success of GW170817 provided greater constraints on what should be searched for, demonstrating the importance of quieter, potentially off-axis GRBs (Burns et al. 2018; Mooley et al. 2018; von Kienlin et al. 2019).

As a GW event, GW170817 was very loud and would not have been missed even without the multi-messenger electromagnetic observations (Abbott et al. 2017b). However, multi-messenger astronomy provides the possibility of combining data sets from different observatories to promote events that would not have been convincing on their own into solid astrophysical candidates; for example, the TeV-energy neutrino IceCube-170922A coincident with a gamma-ray flare from a blazar (Aartsen et al. 2018). This is because a coincident search between two observation sets can substantially reduce the background that exists in either set independently.

In this Letter we develop a method to perform such coincident multi-messenger searches using GW and gamma-ray data. We demonstrate its performance on open archival data from the Advanced Laser Interferometer Gravitational-Wave Observatory (LIGO)'s first observing run (O1) and coincident *Fermi*-GBM data. We specifically target sub-threshold candidates that would not be significant in either individual data set, but also include autonomously detected GRBs. We restrict our search to BNS systems that are similar to the already observed GW170817. Previous searches of these data sets have either looked for weak GW signals associated with autonomously detected GRBs (Abbott et al. 2017d), or have used sub-threshold GW candidates without imposing the constraint that they should be BNS systems (Burns et al. 2019).

The LIGO Scientific and Virgo Collaborations have released a list of candidate triggers with a false alarm rate that is less than 1 per 30 days (Abbott et al. 2018). Within this set, the most confident GW detections are seen at false alarm rates less than one per hundred years. Over the past decade, GBM has provided thousands of autonomously generated triggers (Goldstein et al. 2017). During O1, 42 GRBs were seen by a number of different detectors (Hurley et al. 2003; Gruber et al. 2014; Lien et al. 2016), with 15 of these being the short/hard type believed to be associated with BNS mergers (Abbott et al. 2017d). Nearby short GRBs may not be especially luminous (-Burns et al. 2016; Abbott et al. 2017a). Although GW detectors do not currently have the range needed to observe all GRBs, the observation of GW170817 has raised the importance of studying nearby and potentially less-energetic GRBs. GW170817 was observed to be between two and six orders of magnitude less energetic than other short GRBs (Abbott et al. 2017a).

Based on the estimated viewing angle of GW170817, it is reasonable to assume that BNSs produce GRBs that are beamed and may be observable within a cone of $\sim 30^{\circ}$ (Schutz 2011; Fong et al. 2015; Finstad et al. 2018). With this restriction on inclination, we estimate the sky-averaged sensitive distance of the GW search to be 140 Mpc during the time that both LIGO detectors were observing, and 100 Mpc in single-detector observing time at a false alarm rate

of 1 per year. Using an approximate rate of BNS mergers of $1000\,\mathrm{Gpc}^{-3}\,\mathrm{yr}^{-1}$ (Abbott et al. 2018), the expected number of BNSs in this volume during O1 is ∼1.98, of which we expect 0.27 events to be beamed toward Earth. Our joint GW-GRB search finds one potential coincident candidate at a false alarm rate of 1 in 13 yr and source-frame chirp mass $\sim 1.30\,M_{\odot}$. By comparing the expected number of signals to the search-estimated number of false alarms, we estimate that this candidate has a 1 in 4 chance of being astrophysical.

2. Combined Search for GW-GRB Coincidences

We search for multi-messenger GW-GRB candidates by correlating sub-threshold GW candidates from the public 1-OGC catalog (Nitz et al. 2019a) including single-detector GW candidates with GRB candidates from the combined set of public *Swift*-BAT (Lien et al. 2016) and *Fermi*-GBM candidates (Gruber et al. 2014; von Kienlin et al. 2014; Bhat et al. 2016), as well as our own set of sub-threshold candidates derived from a straightforward analysis of the archival *Fermi*-GBM data. This analysis is targeted at finding GW-GRB coincidences produced by BNS mergers that are similar to GW170817 and GRB 170817A. Using a simulated set of GW signals, we estimate that, relative to a GW search alone, this analysis is able to achieve a ∼20% improvement in sensitive distance. This is comparable to the coherent follow-up of GRBs in Abbott et al. (2017d) and Williamson et al. (2014).

2.1. GW Candidates

The 1-OGC catalog (Nitz et al. 2019a) contains candidate mergers during times when the LIGO instruments were both observing, and is particularly suitable for multi-messenger follow-up due to the low threshold for candidate inclusion. We select candidates from this catalog that are consistent with the expected population of BNSs (as discussed below) and use the public LIGO data (Vallisneri et al. 2015) to produce sky localizations for each GW candidate. In addition to candidate events from the 1-OGC catalog, which only includes candidates when both LIGO instruments were observing, we also search times when only one of the two LIGO instruments (Hanford or Livingston) was observing. While single-detector GW observations are typically difficult to confidently claim on their own, they can be confirmed by a GRB counterpart. Coincident LIGO observing time accounts for ∼48 days of data; single-detector observing time adds an additional ∼44 days.

Considering astrophysical observations, including GW170817, we target BNSs with component masses $1.33 \pm 0.09\,M_{\odot}$ (Özel & Freire 2016). The 1-OGC catalog records the detector-frame component masses $m_{1,2}$ and aligned dimensionless spin components $\chi_{1z,2z} = S_{1z,2z}/m_{1,2}^2$ of the GW template waveform associated with each candidate event. We select candidates that are consistent with this population by placing constraints on the chirp mass $\mathcal{M} = (m_1 m_2)^{3/5}/(m_1 + m_2)^{1/5}$ and effective spin $\chi_{\mathrm{eff}} = (\chi_{1z} m_1 + \chi_{2z} m_2)/(m_1 + m_2)$ (Ajith 2011). These parameters are more accurately measured than the component masses and spins directly (Cutler & Flanagan 1994; Ohme et al. 2013). We find the detector-frame constraints $1.03 < \; < 1.36 M_{\odot}$ and $|\chi_{\mathrm{eff}}| < 0.2$ are effective at recovering a simulated population of sources and allows for a 2σ deviation in the masses. This range also accounts for the average shift in the observed masses due to cosmological redshift.

Each candidate event from the 1-OGC sample was observed by both LIGO detectors and already has an assigned ranking statistic $\tilde{\rho}_c$ that is proportional to signal-to-noise ratio (S/N) under ideal conditions and inversely proportional to the luminosity distance (Nitz et al. 2017, 2019a). There are 3395 1-OGC candidates with $\tilde{\rho}_c > 6.5$ selected by the cuts described in the previous paragraph. We use PyCBC Inference (Biwer et al. 2019; Nitz et al. 2018) to estimate their sky localizations. We fix the component masses and spins of the source binary to those found in the 1-OGC catalog. This is a reasonable approximation because the estimation of the sky localization is largely independent from the other parameters (Singer & Price 2016). For 3% of these candidates the sky-location estimation failed to converge, and instead we use the combined Hanford and Livingston detector response, which is the sensitivity of the detectors to a given sky location. Closer inspection of many of these cases indicated that they lay in stretches of time with non-stationary data.

For single-detector candidates, we select triggers that lie in our chosen parameter space, are the loudest candidate within 10 s, and that have re-weighted S/N $\tilde{\rho}_{H,L} > 7$ (Babak et al. 2013; Nitz et al. 2019a). The sky localization assigned for single-detector candidates is the detector response of its respective LIGO observatory.

2.2. GRB Candidates

We generate our sample of GRBs separately from our set of GW candidates. We include all short GRBs ($T_{90} < 2$ s) reported by both *Swift*-BAT and *Fermi*-GBM from 2015 September through 2016 January (Gruber et al. 2014; von Kienlin et al. 2014; Bhat et al. 2016; Lien et al. 2016). We also include sub-threshold events reported by *Fermi*-GBM during this time.[3] Many of these candidates have been previously searched and found to have no identifiable LIGO counterpart (Abbott et al. 2017d). Because the expected GRB luminosity for a given GW candidate is not well constrained, and indeed subluminous bursts are of interest, we also conduct our own search of *Fermi*-GBM data with lowered thresholds. The aim is to include lower luminosity sources at the expense of the purity of the sample set.

We use archival time-tagged event (TTE) data from *Fermi*-GBM that consists of discrete events with a time and energy range from each of the 12 NaI and two BGO detectors (Meegan et al. 2009). GRBs similar to GW170817 are bright in the range 50–300 keV (von Kienlin et al. 2019) so we combine the recorded photon counts within this energy range from all 12 NaI detectors. We do not include the BGO detectors as they focus on a higher energy range. For each event we calculate the combined number of photon counts within a ±0.1 s window. As the overall observed count flux can vary significantly over tens of seconds, we normalize our results by subtracting out the locally measured mean and dividing by the standard deviation. To measure the local mean and standard deviation, we limit to times within ±4 s centered around each event and exclude time within ±0.5 s to prevent a candidate GRB from biasing the estimates. We finally threshold on this normalized count excess, C_{GBM}.

[3] https://gammaray.nsstc.nasa.gov/gbm/science/sgrb_search.html

We find thresholding at $C_{\rm GBM} > 5.5$ includes all previously identified *Fermi* short GRBs in our sample set. At this threshold we identify ∼1 candidate GRB every 3 hr. The aim of this threshold is to minimize false negatives while preserving the statistical power of the analysis, and so it necessarily reduces the purity of our GRB sample. For comparison, the lowest value of $C_{\rm GBM}$ assigned to a previously identified GRB is ∼7.8 and GRB 170817 A would have been ∼10.5.

A sky localization is assigned to to each candidate GRB. For any event that was previously reported, we use the published value and uncertainty. It is left to future work to measure detailed sky localizations for candidate GRBs identified with our sub-threshold analysis. In this analysis we assign them an isotropic sky localization. In all cases, we exclude directions that are occulted by the Earth from the perspective of *Fermi*.

2.3. Combining Gravitational and Gamma-Ray Candidates

We look for temporal coincidences between our two independent GW and GRB candidate sets. We allow a GRB to occur 0–3.4 s after the GW merger time (which happens to be broadly consistent with previous searches; Abadie et al. 2010). As we do not expect a GRB to arrive before an associated GW, this sets the lower bound on the time window. Astrophysical models are insufficient to constrain the upper time window, so we choose to use a symmetrical ±1.7 s window around the 1.7 s time delay between GW170817 and GRB 170817A. Given the rate of GW and GRB candidates in our sample, this window corresponds to expecting one GRB-GW candidate by accidental coincidence in the 48 days when both LIGO instruments were observing.

We rank candidates according to their GW likelihood and the agreement between the GW and GRB sky localization. This takes the form

$$\rho^2_{\rm gw+grb} = \rho^2_{\rm gw} + 2\log(B_{\rm loc}) \quad (1)$$

where $\rho_{\rm gw}$ is the S/N-like statistic associated with a given GW candidate event, and $B_{\rm loc}$ is the spatial Bayes factor employed by Ashton et al. (2018), which measures the agreement between the GW and GRB sky localizations. We do not include an explicit ranking of GRB candidates based on their flux due to the uncertainty in the relation between GW amplitude and GRB flux.

Under the assumption that the non-astrophysical backgrounds of GRB and GW detectors are not correlated in time, we determine the background of accidental coincidences by shifting the GRB candidates in time. We create 10^4 time-shifted analyses, which allows us to measure the false alarm rate as a function of our ranking statistic $\rho_{\rm gw+grb}$. We estimate separate backgrounds for time when a single LIGO detector is operating and when both LIGO instruments are observing.

3. Observational Results

Figure 1 summarizes the results of our analysis. We find no candidate events during times when only a single LIGO instrument was observing, and two candidate events during times when both instruments were observing. The loudest candidate was observed at a false alarm rate of 1 per 13 yr. Taking into account the ∼92 days of data analyzed, which includes single-detector operation, this event has a statistical significance of 2.0σ. The second candidate is observed at a lower significance, and is consistent with the expected accidental coincident rate.

The candidate event, 1-OGC 151030, occurred on 2015 October 30, at 6:41:53 UTC (GPS time 1130222530). The event was recovered with S/N 5.7 in Livingston and 2.4 ms later with S/N 6.0 in Hanford. This was followed by a peak of $C_{\rm GBM} \sim 5.7$ in the observed gamma-ray counts 3.1 s later. The observed counts from *Fermi*-GBM along with the S/N time series from the GW template that recovered this candidate are shown in Figure 2.

We estimate the probability that 1-OGC 151030 is astrophysical in origin by comparing the expected number of signal and noise events with similar $\rho_{\rm gw+grb}$. We assume that the rate of BNS mergers is $1000\,{\rm Gpc}^{-3}\,{\rm yr}^{-1}$, which is consistent with Abbott et al. (2018), and that the sources are uniformly distributed in volume. The fraction of sources that are detectable as a function of $\rho_{\rm gw+grb}$ is determined by searching for simulated GW signals. We restrict our search to the portion of this population that could plausibly be visible with *Fermi*-GBM by constraining the source inclination of our simulated population to be less than 30°, and by taking into account the fact that nearly half of the potential sources may be missed due to detector downtime and blockage by the Earth. With these considerations, we count the number of signals that would be detected with $\rho_{\rm gw+grb}$ within ±0.1 of 1-OGC 151030 and compare to the number of background samples obtained by the search in the same range. We find that the expected number is ∼0.018 and ∼0.0064 noise and signal samples, respectively. This means that 1 in 4 candidates with this ranking statistic value would be astrophysical in origin. Following the same procedure, our second-most significant candidate would have a 1 in 25 chance of being astrophysical in origin.

An examination of the *Fermi*-GBM counts in the 12 individual NaI detectors does not reveal a single detector primarily responsible for the observed excess. A time-frequency representation of the LIGO data is shown in Figure 3. While no strong transient noise similar to that which occurred during GW170817 is evident, we cannot rule out the possibility of some non-stationary noise affecting the data during this time.

We estimate posterior probabilities of the event's GW parameters by performing a Bayesian analysis on the LIGO data with PyCBC Inference (Biwer et al. 2019; Nitz et al. 2018) and using the TaylorF2 post-Newtonian waveform (Sathyaprakash & Dhurandhar 1991; Droz et al. 1999; Blanchet 2002; Faye et al. 2012) to model the GW. For this analysis we use a uniform prior in component masses $m_{1,2} \in [1, 3)M_\odot$, which spans the entire range of known neutron-star masses (Özel & Freire 2016). The dimensionless spins of each component $\chi_{1,2}$ are constrained to be aligned with the orbital-angular momentum with a prior that is uniform in (−0.4, 0.4). This choice is consistent with the fastest-known spinning neutron star (Hessels et al. 2006). The tidal deformability parameters $\Lambda_{1,2}$ of the components are varied independently of each other, with a prior uniform in (0, 5000). We use a prior isotropic in binary orientation and uniform in volume between 5 and 500 Mpc. A uniform prior spanning $t_c \pm 0.1$ s is used for the coalescence time, where t_c is the coalescence time estimated by the search. To measure likelihood, 128 s of data spanning $t_c - 110$ s to $t_c + 18$ s are filtered between 20 and 2048 Hz. The power spectral density of each detector is estimated using

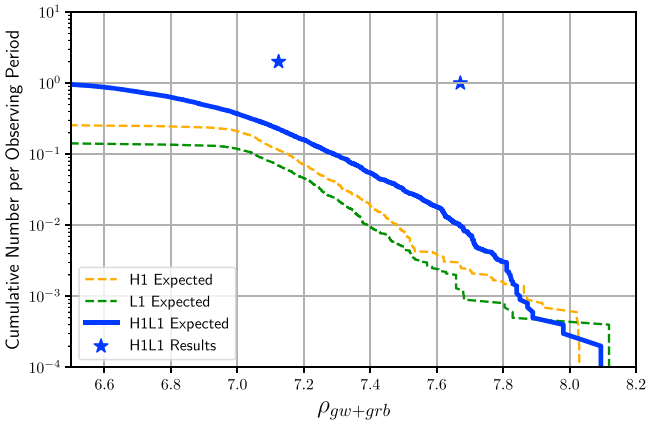

Figure 1. Results from our search for GW-GRB coincidences. The lines show the cumulative number of expected accidental coincidences during times when only LIGO-Hanford (orange), only LIGO-Livingston (green), and both LIGO instruments (blue) are observing as a function of our ranking statistic $\rho_{\mathrm{gw-grb}}$. No candidate events were found during times when a single LIGO detector was observing. The two candidates found when both LIGO instruments were observing are shown with blue stars. The most significant is 1-OGC 151030. We expect an accidental candidate at least as significant as 1-OGC 151030 once in 100 48 day analyses. This corresponds to a false alarm rate of 1 in 13 yr.

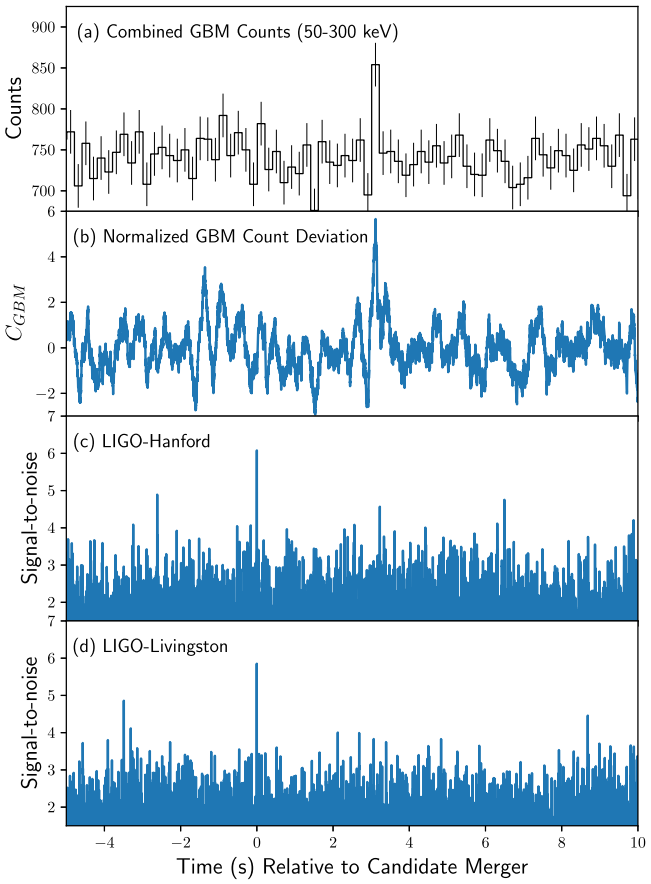

Figure 2. Time series results from the *Fermi*-GBM and the LIGO observatories at the time of 1-OGC 151030. (a) shows a simple histogram of the GBM data from all 12 NaI detectors with a bin width of 0.2 s. (b) shows the normalized statistic C_{GBM} that we use to determine the presence of a gamma-ray excess. We impose a threshold of $C_{\mathrm{GBM}} > 5.5$ to determine our population of low significance samples. (c) and (d) show the signal-to-noise time series for the GW template waveform used to find this candidate. Two peaks in the GW S/N are visible at nearly the same time followed by a small peak in the normalized deviation in GBM counts 3.1 s later.

Welch's method with 512 s of data centered on the event. No marginalization over calibration uncertainty is performed.

The results of the parameter estimation are shown in Figures 4 and 5. Figure 4 shows the marginal posterior distributions of the source-frame chirp mass $\mathcal{M}^{\mathrm{src}}$, mass ratio q, effective spin χ_{eff}, inclination ι, and luminosity distance d_{L}. The median and 90% credible intervals for each parameter are quoted above the 1D marginal plots, with the exception of the inclination angle (due to the bimodal posterior) and the mass ratio (as it is largely unconstrained). To estimate $\mathcal{M}^{\mathrm{src}}$ from the observed, detector-frame chirp mass, we assume a standard ΛCDM cosmology (Planck Collaboration et al. 2016). Figure 5 shows a 2D marginal distribution of the sky location. The tidal parameters $\Lambda_{1,2}$ (not shown) are not constrained, which is expected for low S/N sources.

We also perform parameter estimation separately on data from each GW detector. The single-detector S/Ns recovered by this analysis are consistent with the coherent S/N of the signal. However, the detector-frame chirp mass posterior shows multiple peaks in the Livingston detector. This may indicate the presence of non-stationary or non-Gaussian noise in the Livingston detector. To determine if such peaks can be observed with a known signal in similar data, we repeated the analysis on a simulated signal with similar parameters added to the data, offset by $t_c + 0.157$ s. Because we find similar peaks in the recovered chirp mass of the simulated signal, the 1-OGC 151030 Livingston results do not necessarily rule out an astrophysical source.

The degeneracy between inclination angle and luminosity distance is evident in the right plot of Figure 4. The bimodal posterior of the inclination angle is typical when the data is uninformative about the viewing angle. This is expected for BNSs for which no independent redshift information is available (Chen et al. 2018). The degeneracy leads to a larger uncertainty in the luminosity distance. However, if we assume that the viewing angle is $<30^{\circ}$ in order to be detected by *Fermi*-GBM, then we obtain a luminosity distance of 224^{+88}_{-78} Mpc.

By their very nature, sub-threshold detections will dominate the population of the most distant signals. As such, these sub-threshold events will always provide the strongest constraints on the speed of gravity. In our search we have explicitly assumed that a GRB trigger should lie within 3.4 s of a GW trigger in order to be coincident. Assuming, however, that 1-OGC 151030 is a real astrophysical event seen in both GWs and gamma-rays, we can use the arrival times to constrain the speed of gravity relative to the speed of light, $\delta v = v_{\mathrm{GW}} - v_{\mathrm{EM}}$. Following the method of Abbott et al. (2017a) and using a 90% lower bound on the distance of 116 Mpc, we obtain

$$-6 \times 10^{-16} \leqslant \frac{\delta v}{v_{\mathrm{EM}}} \leqslant 3 \times 10^{-16}. \quad (2)$$

The upper (positive) bound is a factor 2 stronger than Abbott et al. (2017a) and the lower (negative) bound is a factor 5 stronger. This improvement is mainly due to the larger luminosity distance of the signal compared to GW170817.

4. Discussion

We search for BNS mergers that are observable both by their GW and associated GRB emission. We have combined the likelihood that these multi-messenger candidates are associated with a true GW signal and the likelihood of sky localization

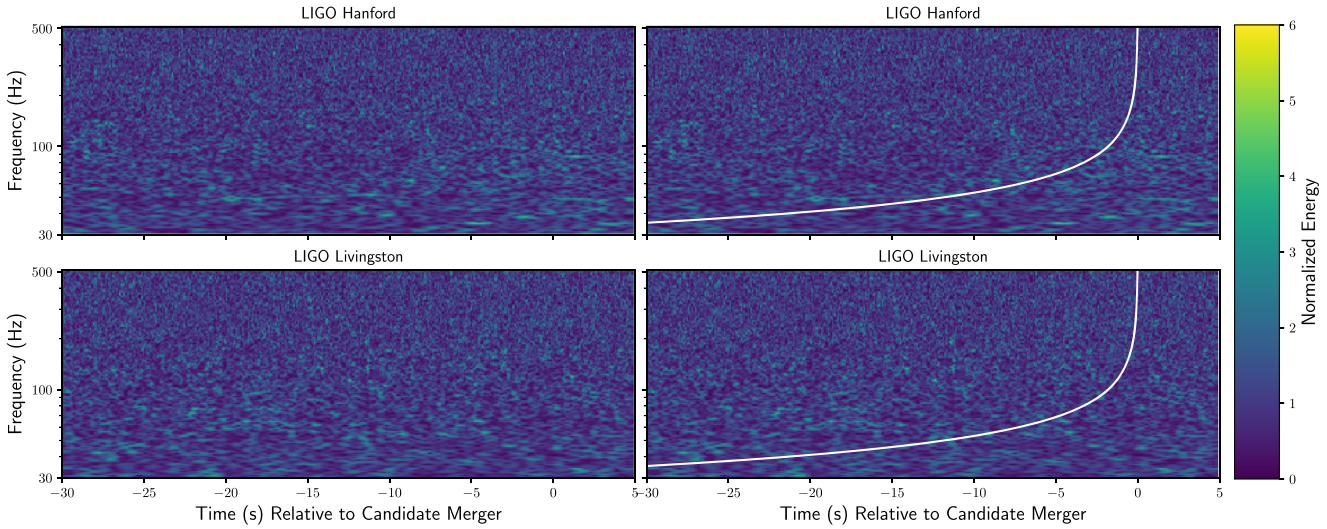

Figure 3. Time-frequency representations of the GW data using the Q-transform ($Q = 100$) around the time of the 1-OGC 151030 candidate. Upper (lower) panels show data from the LIGO-Hanford (Livingston) observatory. No loud transient noise similar to that observed during GW170817 is visible. The left panels show the raw data alone. The right panels overlay the same data with a track of a GW signal with the parameters of 1-OGC 151030 to guide the eye. No visible track is expected in the raw data for quiet signals.

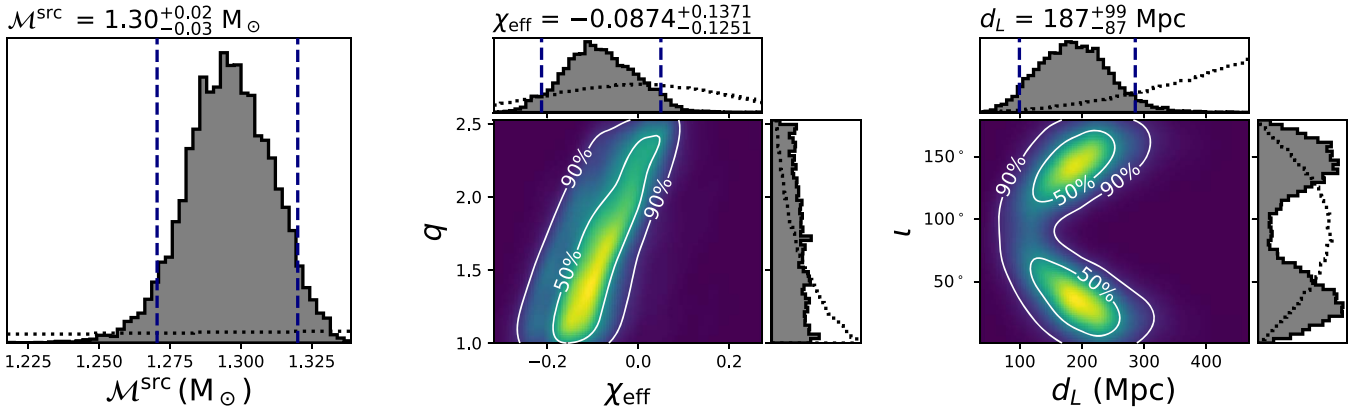

Figure 4. Marginal posterior distributions of the source chirp mass $\mathcal{M}^{\rm src}$ (left panel), mass ratio q (which we define to be $\geqslant 1$) and effective spin $\chi_{\rm eff}$ (middle panel), and inclination ι and luminosity distance $d_{\rm L}$ (right panel). The vertical, dashed blue lines show the 5th and 95th percentiles of the 1D marginal posteriors. The dotted black lines show the priors. The source-frame chirp mass is determined from the observed (detector-frame) chirp mass by $\mathcal{M}/(1+z)$, where the redshift z is determined from $d_{\rm L}$ using a standard ΛCDM cosmology (Planck Collaboration et al. 2016).

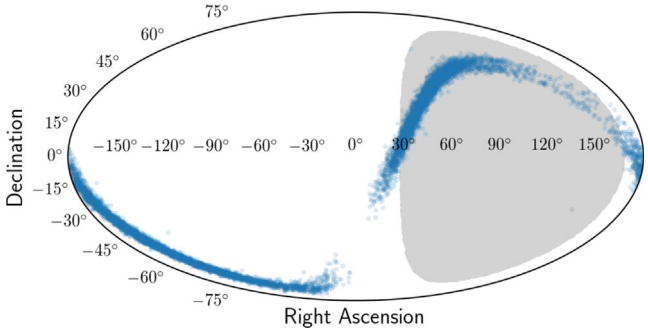

Figure 5. Sky localization for 1-OGC 151030. Samples from the posterior probability are shown in blue. The gray region shows the portion of the sky occulted by the Earth from the perspective of the *Fermi* satellite at the time of the event. If 1-OGC 151030 is a real GW-GRB observation, then it cannot have come from the 40% of the GW sky localization that is blocked by the Earth. This corresponds to $B_{\rm loc} \sim 0.8$.

agreement with a GRB source. With future observations, this methodology could be further improved by including the likelihood that a GRB candidate is astrophysical for sub-threshold GRB events along with a model that relates the GW and GRB observables, such as GW observed masses and GRB energy spectrum.

A major uncertainty in the sensitivity of this analysis is the unknown selection bias of the GRB candidates. If this population of GRB candidates is just as likely to contain the counterpart to a sub-threshold GW event as a clearly detected GW, then the overall sensitive distance is 20% greater, corresponding to 70% in volume, than a GW search alone. This indicates that approximately 40% of all GW-GRB events that could be observed will only be found by this kind of search. However, if our population of GRBs does not contain the possible counterparts to quiet GW events, then the practical sensitivity of this search will be lower than expected. Given the rate of short GRBs, it is beneficial to examine lower threshold candidates that cannot necessarily be discerned as GRBs on their own. We have shown that setting a threshold such that we recover candidates at a false alarm rate of 1 per 3 hr still allows the search to reach our target sensitivity. Methods discussed in Blackburn et al. (2015) and Goldstein et al. (2016) demonstrate that coherently combining the *Fermi*-GBM data can increase

sensitivity to weak sources. Future work may significantly improve the purity of our GRB sample and include more detailed information that can be correlated with GW observations.

The main advantage of a joint analysis is the reduction in non-astrophysical background compared to a GW or GRB search alone. This background reduction primarily arises from the requirement that a GW and GRB candidate occur in close temporal proximity. Our analysis also takes into account the agreement between GW and GRB localizations when available. However, this is not a strict constraint due to the large uncertainty in source location for most of our sample. Improved localization for the majority of our candidates would further reduce the background. In the case of 1-OGC 151030, the original false alarm rate of this candidate from the 1-OGC analysis was 1 per 2 hr (Nitz et al. 2019a). If we restrict our analysis to just BNS-like sources, the false alarm rate would have been 1 per 2 days. By combining GW-only analysis with information from *Fermi*-GBM, this candidate was promoted to 1 per 13 yr. Improved localization of the GRB component of this candidate may be able to further strengthen or weaken the association between the GW and GRB observations.

Even if the event 1-OGC 151030 is not a true GW-GRB observation, the prospects for detecting such signals in the near future in data from the second or third LIGO observing run seem compatible with more optimistic scenarios (Howell et al. 2018). In the years to come, the combination of information from different astronomical observations will be of increasing importance and will likely include not just GW and gamma-ray observations, but also other parts of the electromagnetic spectrum, neutrinos, and cosmic rays (Branchesi 2016). In particular, surveys of kilonova candidates with the Large Synoptic Survey Telescope may provide another population which could be further correlated with GW candidates and increase the reach of multi-messenger searches (Andreoni et al. 2018; Setzer et al. 2019).

To aid follow-up, we make available supplementary materials that include sky localizations for our GW candidates and the posterior samples for 1-OGC 151030 (Nitz et al. 2019b).

We thank Sylvia Zhu, Eric Burns, Sebastian Khan, Duncan Brown, Tito Dal Canton, and Thomas Dent for their feedback. We acknowledge the Max Planck Gesellschaft and the Atlas cluster computing team at AEI Hanover for support. This research has made use of data, software, and/or web tools obtained from the Gravitational Wave Open Science Center (https://www.gw-openscience.org), a service of LIGO Laboratory, the LIGO Scientific Collaboration and the Virgo Collaboration. LIGO is funded by the U.S. National Science Foundation. Virgo is funded by the French Centre National de Recherche Scientifique (CNRS), the Italian Istituto Nazionale della Fisica Nucleare (INFN) and the Dutch Nikhef, with contributions by Polish and Hungarian institutes.

ORCID iDs

Alexander H. Nitz https://orcid.org/0000-0002-1850-4587
Alex B. Nielsen https://orcid.org/0000-0001-8694-4026
Collin D. Capano https://orcid.org/0000-0002-0355-5998

References

Aartsen, M. G., Ackermann, M., Adams, J., et al. 2018, Sci, 361, eaat1378
Abadie, J., Abbott, B. P., Abbott, T. D., et al. 2010, ApJ, 715, 1453
Abbott, B. P., Abbott, R., Abbott, T. D., et al. 2017a, ApJL, 848, L13
Abbott, B. P., Abbott, R., Abbott, T. D., et al. 2017b, PhRvL, 119, 161101
Abbott, B. P., Abbott, R., Abbott, T. D., et al. 2017c, ApJL, 848, L12
Abbott, B. P., Abbott, R., Abbott, T. D., et al. 2017d, ApJ, 841, 89
Abbott, B. P., Abbott, R., Abbott, T. D., et al. 2018, arXiv:1811.12907
Ajith, P. 2011, PhRvD, 84, 084037
Andreoni, I., Anand, S., Bianco, F. B., et al. 2018, arXiv:1812.03161
Ashton, G., Burns, E., Canton, T. D., et al. 2018, ApJ, 860, 6
Babak, S., Biswas, R., Brady, P., et al. 2013, PhRvD, 87, 024033
Bhat, P. N., Meegan, C. A., von Kienlin, A., et al. 2016, ApJS, 223, 28
Biwer, C. M., Capano, C. D., De, S., et al. 2019, PASP, 131, 024503
Blackburn, L., Briggs, M. S., Camp, J., et al. 2015, ApJS, 217, 8
Blanchet, L. 2002, LRR, 5, 3
Branchesi, M. 2016, JPhCS, 718, 022004
Burns, E., Connaughton, V., Zhang, B.-B., et al. 2016, ApJ, 818, 110
Burns, E., Veres, P., Connaughton, V., et al. 2018, ApJL, 863, L34
Burns, E., Goldstein, A., Hui, C. M., et al. 2019, ApJ, 871, 90
Chen, H.-Y., Vitale, S., & Narayan, R. 2018, arXiv:1807.05226
Cutler, C., & Flanagan, E. E. 1994, PhRvD, 49, 2658
Droz, S., Knapp, D. J., Poisson, E., & Owen, B. J. 1999, PhRvD, 59, 124016
Faye, G., Marsat, S., Blanchet, L., & Iyer, B. R. 2012, CQGra, 29, 175004
Finstad, D., De, S., Brown, D. A., Berger, E., & Biwer, C. M. 2018, ApJL, 860, L2
Fong, W.-f., Berger, E., Margutti, R., & Zauderer, B. A. 2015, ApJ, 815, 102
Goldstein, A., Burns, E., Hamburg, R., et al. 2016, arXiv:1612.02395
Goldstein, A., Veres, P., Burns, E., et al. 2017, ApJL, 848, L14
Gruber, D., Goldstein, A., Weller von Ahlefeld, V., et al. 2014, ApJS, 211, 12
Hessels, J. W., Ransom, S. M., Stairs, I. H., et al. 2006, Sci, 311, 1901
Howell, E. J., Ackley, K., Rowlinson, A., & Coward, D. 2018, arXiv:1811.09168
Hurley, K., Cline, T., Mitrofanov, I., et al. 2003, in AIP Conf. Proc. 662, Gamma-Ray Burst and Afterglow Astronomy 2001, ed. G. R. Ricker & R. K. Vanderspek (Melville, NY: AIP), 473
Lien, A., Sakamoto, T., Barthelmy, S. D., et al. 2016, ApJ, 829, 7
Meegan, C., Lichti, G., Bhat, P. N., et al. 2009, ApJ, 702, 791
Mooley, K. P., Frail, D. A., Dobie, D., et al. 2018, ApJL, 868, L11
Nitz, A. H., Capano, C., Nielsen, A. B., et al. 2019a, ApJ, 872, 195
Nitz, A. H., Capano, C., & Nielsen, A. B. 2019b, gw-grb o1 analysis datarelease, www.github.com/gwastro/o1-gwgrb, GitHub
Nitz, A. H., Dent, T., Dal Canton, T., Fairhurst, S., & Brown, D. A. 2017, ApJ, 849, 118
Nitz, A. H., Harry, I. W., Willis, J. L., et al. 2018, PyCBC Software, https://github.com/gwastro/pycbc, GitHub, Zenodo, doi:10.5281/zenodo.596388
Ohme, F., Nielsen, A. B., Keppel, D., & Lundgren, A. 2013, PhRvD, 88, 042002
Özel, F., & Freire, P. 2016, ARA&A, 54, 401
Planck Collaboration, Ade, P. A. R., Aghanim, N., et al. 2016, A&A, 594, A13
Sathyaprakash, B. S., & Dhurandhar, S. V. 1991, PhRvD, 44, 3819
Schutz, B. F. 2011, CQGra, 28, 125023
Setzer, C. N., Biswas, R., Peiris, H. V., et al. 2019, MNRAS, 485, 4260
Singer, L. P., & Price, L. R. 2016, PhRvD, 93, 024013
Vallisneri, M., Kanner, J., Williams, R., et al. 2015, JPhCS, 610, 012021
von Kienlin, A., Meegan, C. A., Paciesas, W. S., et al. 2014, ApJS, 211, 13
von Kienlin, A., Veres, P., Roberts, O. J., et al. 2019, arXiv:1901.06158
Williamson, A. R., Biwer, C., Fairhurst, S., et al. 2014, PhRvD, 90, 122004